Electrochemical Materials and Technologies

LETTER

Electrochemical Materials and Technologies

eISSN: 2949-0561

Cite this: Electrochem. Mater. Technol. 2 (2023) 20232015

Heterovalent and isovalent doping of bilayer proton-conducting perovskite $SrLa_2Sc_2O_7$

Nataliia Tarasova [a *]

Received: 17 July 2023
Accepted: 31 July 2023
Published online: 1 August 2023

DOI: 10.15826/elmattech.2023.2.015

Perovskite or perovskite-related structural materials are widely studied for their many functional properties. They can be used as components of energy sources such as solid oxide fuel cells. Along with classical perovskites, layered perovskites can also carry out high-temperature proton transport and are promising materials for use in electrochemical power engineering. In this paper, the possibility of heterovalent and isovalent doping of La and Sc sublattices of bilayer perovskite $SrLa_2Sc_2O_7$ was made for the first time. It was shown that electrical conductivity increases in the row of bilayer perovskites $SrLa_2ScInO_7$ – $SrLa_2Sc_2O_7$ – $BaLa_2In_2O_7$ – $BaNd_2In_2O_7$.

keywords: layered perovskite; oxygen-ion conductivity; proton conductivity; hydrogen energy; Ruddlesden-Popper structure

1. Introduction

Perovskite or perovskite-related structural materials are widely studied for their many functional properties. Some of these applications are solar cells [1–4], light-emitting diodes [5], semiconductor lasers [7], photovoltaic [8, 9] and optoelectronic applications [10], and solid oxide fuel cells and electrolyzers [11–15]. Solid oxide fuel cells are energy sources. They work by converting energy from chemical reactions into electricity. This is the field of hydrogen energy. It is very promising, both in terms of energy resource availability and the environment [16–18]. A solid oxide fuel cell consists of several components, including electrolyte, electrodes, interconnector and glass sealant. The electrolyte material can be an oxygen ion conductor or a proton conductor. Doped barium zirconate is the most studied electrolyte material for proton conducting solid oxide fuel cells [19]. It crystallises in the classic perovskite ABO_3 structure. However, there are a number of problems with the use of these materials, including low grain boundary conductivity, poor sinterability and low oxygen vacancy concentrations created by an accepter-doping mechanism [20–24]. Therefore, the search for new proton-conducting materials is necessary.

The ability of layered perovskites $AA'_nB_nO_{3n+1}$ to transport oxygen ions [25–32] and protons [33–38] was demonstrated a few years ago. The monolayer perovskites $AA'BO_4$ such as $BaLaInO_4$, $SrLaInO_4$, $BaNdInO_4$, have a crystal lattice capable of doping both Ba/La and In sublattices [39]. The bilayer perovskites $AA'_2B_2O_7$ such as $BaLa_2In_2O_7$ and $BaNd_2In_2O_7$ allow predominantly doping only in the A or A′ sublattices [40–43] (Figure 1). Last year, the possibility of oxygen ion and proton transport was proved for the bilayer perovskite $SrLa_2Sc_2O_7$ [44]. This paper first explores the possibility of heterovalent and isovalent doping of La and Sc sublattices.

a: Institute of High Temperature Electrochemistry of the Ural Branch of the Russian Academy of Sciences, Yekaterinburg 620066, Russia

* Corresponding author: Natalia.Tarasova@urfu.ru

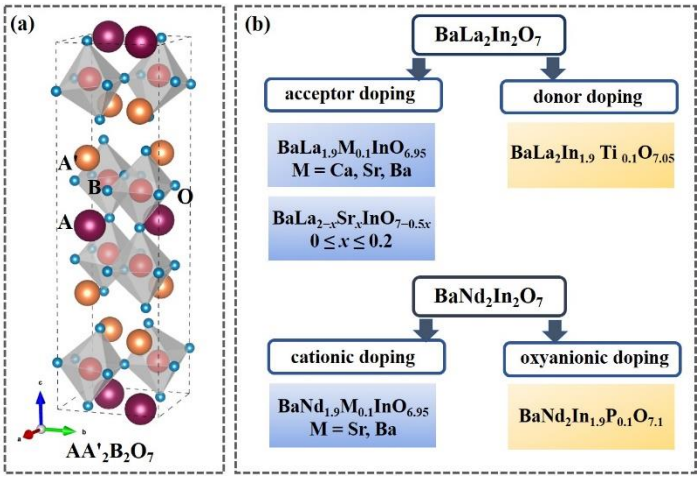

Figure 1 The crystal structure of a bilayer perovskite with the general formula $AA'_2B_2O_7$ (a) and the scheme of doping of layered perovskites $BaLa_2In_2O_7$ and $BaNd_2In_2O_7$ (b).

2. Experimental

The compositions $SrLa_2Sc_2O_7$, $SrLa_{1.9}Ca_{0.1}Sc_2O_{6.95}$, $SrLa_{1.9}Sr_{0.1}Sc_2O_{6.95}$, $SrLa_{1.9}Ba_{0.1}Sc_2O_{6.95}$, $SrLa_2Sc_{1.9}In_{0.1}O_7$, $SrLa_2Sc_{1.9}Gd_{0.1}O_7$, $SrLa_2Sc_{1.9}Y_{0.1}O_7$, $SrLa_2Sc_{1.9}Ti_{0.1}O_{7.05}$ and $SrLa_2ScInO_7$ were prepared by the solid state method. The powders of the starting reagents $BaCO_3$, $SrCO_3$, $CaCO_3$, Sc_2O_3, La_2O_3, In_2O_3, Y_2O_3, Gd_2O_3, TiO_2 (all 99.99 % purity, REACHIM, Russia) were dried and used in stoichiometric amounts. An agate mortar was used for grinding. The compositions were heated after each grinding. The annealing was carried out in the temperature range of 800 – 1300 °C with 100 °C step.

The phase identification of the obtained compositions was carried out using the Bruker Advance D8 Cu *Kα* diffractometer. The thermogravimetry (TG) was made using STA 409 PC Netzsch Analyser. The heating of initially hydrated samples was made at the temperature range of 40 – 1100 °C with the rate of 10 °C/min under a flow of dry Ar. The preliminary hydrated samples were obtained by slow cooling from 1000 to 150 °C (1 °C/min) under a flow of wet Ar (99.999 % purity, $pH_2O = 2 \cdot 10^{-2}$ atm). The Ar atmosphere was used to avoid any carbonization of the sample.

The electrical conductivity was measured with an impedance spectrometer Z-1000P, Elins, RF. The investigations were carried out from 1000 to 200 °C with a cooling rate of 1 °/min under dry air or dry Ar. The dry gas (air or Ar) was prepared by circulating the gas through P_2O_5 ($pH_2O = 3.5 \cdot 10^{-5}$ atm). The wet gas (air or Ar) was obtained by bubbling the gas at room temperature first through distilled water and then through a saturated solution of KBr ($pH_2O = 2 \cdot 10^{-2}$ atm).

3. Results and discussions

In this work, the heterovalent (acceptor) doping of the lanthanum sublattice $SrLa_{1.9}M_{0.1}Sc_2O_{6.95}$ (M = Ca, Sr, Ba) and the heterovalent (donor) doping $SrLa_2Sc_{1.9}Ti_{0.1}O_{7.05}$ and the isovalent doping $SrLa_2Sc_{1.9}M'_{0.1}O_7$ (M' = In, Gd, Y) and $SrLa_2ScInO_7$ of the scandium sublattice were provided. The XRD-analysis showed that only two compositions $SrLa_2Sc_2O_7$ and $SrLa_2ScInO_7$ were obtained as single phases. Figure 2 represents the analysis of XRD-data for $SrLa_2ScInO_7$ composition. Both undoped $SrLa_2ScInO_7$ and doped $SrLa_2ScInO_7$ compositions are indexed in the ortorombic symmetry (space group *Fmmm*). The lattice parameters are presented in Table 1.

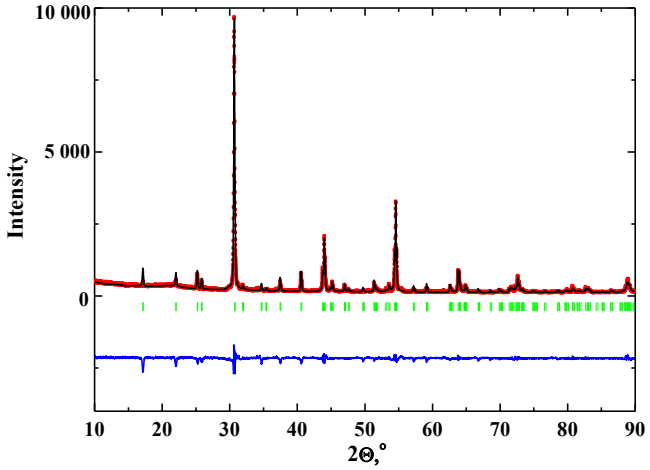

Figure 2 XRD-patterns for the composition $SrLa_2ScInO_7$.

Table 1 – Unit cell parameters and volume of $SrLa_2ScInO_7$ and $SrLa_2ScInO_7$ compositions.

Composition	*a*, Å	*b*, Å	*c*, Å	V_{cell}, Å^3
$SrLa_2Sc_2O_7$	5.7811	5.7381	20.5342	681.171
$SrLa_2ScInO_7$	5.8172	5.8139	20.6772	699.345

Table 2 – Phase composition of obtained samples.

Nominal composition	Phase composition
$SrLa_{1.9}Ca_{0.1}Sc_2O_{6.95}$	$SrLa_{1.9}Ca_{0.1}Sc_2O_{6.95}$, La_2O_3
$SrLa_{1.9}Sr_{0.1}Sc_2O_{6.95}$	$SrLa_{1.9}Sr_{0.1}Sc_2O_{6.95}$, La_2O_3
$SrLa_{1.9}Ba_{0.1}Sc_2O_{6.95}$	$SrLa_{1.9}Ba_{0.1}Sc_2O_{6.95}$, La_2O_3
$SrLa_2Sc_{1.9}In_{0.1}O_7$	$SrLa_2Sc_{1.9}In_{0.1}O_7$, La_2O_3
$SrLa_2Sc_{1.9}Gd_{0.1}O_7$	$SrLa_2Sc_{1.9}Gd_{0.1}O_7$, La_2O_3
$SrLa_2Sc_{1.9}Y_{0.1}O_7$	$SrLa_2Sc_{1.9}Y_{0.1}O_7$, La_2O_3
$SrLa_2Sc_{1.9}Ti_{0.1}O_{7.05}$	$SrLa_2Sc_{1.9}Ti_{0.1}O_{7.05}$, $LaScO_3$, La_2O_3, Sc_2O_3

As can be seen, the introduction of indium ions with bigger ionic radius ($r_{Sc^{3+}}$ = 0.745 Å, $r_{In^{3+}}$ = 0.80 Å [45]) leads to the increase in the lattice parameters and unit cell volume. The phase composition of other samples is presented in Table 2.

The graphical representation for the samples with nominal compositions $SrLa_2Sc_{1.9}Gd_{0.1}O_7$ and $SrLa_2Sc_{1.9}Ti_{0.1}O_{7.05}$ is shown in Figure 3. As previously shown for the bilayer perovskites $BaLa_2In_2O_7$ and $BaNd_2In_2O_7$ [42], the donor doping of the indium sublattice is almost non-existent, in contrast to monolayer perovskites. The crystal lattice of bilayer perovskite contains a linkage of two layers of octahedrons in one perovskite layer and is more rigid compared to the monolayer perovskite layered structure where the layers of the perovskite block are one layer of octahedrons. Accordingly, donor doping, which involves the formation of interstitial oxygen in the interoctahedral space, is not realized. It is obvious that the same reason is an explanation for non-single phase of donor-doped compositions based on $SrLa_2Sc_2O_7$. At the same time, the lattice parameters and unit cell volume for $SrLa_2Sc_2O_7$ composition are much smaller than for $BaLa_2In_2O_7$ and $BaNd_2In_2O_7$ compositions (Table 3). We can assume that this decrease can prevent acceptor doping in the lanthanum sublattice, which is inevitably accompanied by a change in the local structure and the formation of point defects.

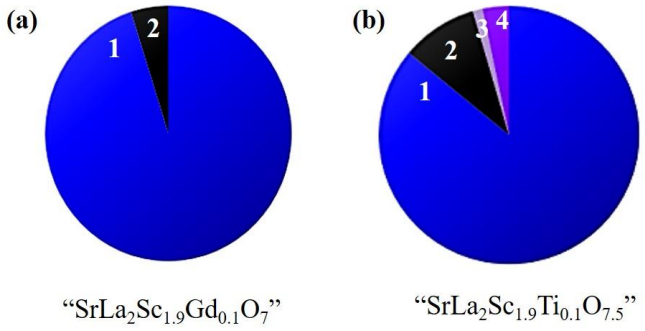

Figure 3 The phase composition (weight ratio) for the samples "$SrLa_2Sc_{1.9}Gd_{0.1}O_7$" (1 - $SrLa_2Sc_{1.9}Gd_{0.1}O_7$, 2 - La_2O_3) and "$SrLa_2Sc_{1.9}Ti_{0.1}O_{7.05}$" (1 - $SrLa_2Sc_{1.9}Ti_{0.1}O_{7.05}$, 2 - $LaScO_3$, 3 - La_2O_3, 4 - Sc_2O_3).

Table 3 – The lattice parameters and unit cell volumes of bilayer perovskites $AA'_2B_2O_7$.

Composition	*a*, Å	*b*, Å	*c*, Å	V_{cell}, Å^3
$SrLa_2Sc_2O_7$	5.7811	5.7381	20.5342	681.171
$BaLa_2In_2O_7$	5.9149	5.9149	20.8465	729.336
$BaNd_2In_2O_7$	5.8916	5.8916	20.4960	710.520

The possibility of interaction with water vapours was investigated using thermogravimetry (TG) and mass spectrometry (MS) measurements. Mass loss occurs at the temperatures below 500 °C (TG curve) and is solely due to the release of water (MS(H_2O) curve). The water uptake for composition $SrLa_2ScInO_7$ is about 0.06 mol H_2O per mol complex oxide (Figure 4), which is slightly more than for composition $SrLa_2Sc_2O_7$ (0.05 mol H_2O [44]). The compositions $BaLa_2In_2O_7$ and $BaNd_2In_2O_7$ are characterised by the water uptake 0.17 and 0.15 mol H_2O per mol complex oxide correspondingly. For the layered perovskites, the possibility of water uptake is due to the presence of enough space between perovskite blocks and rock-salt layers [40]. The increase in the size of this space leads to the increase in the water uptake. Accordingly, the changes in unit cell volume and the changes in this space should lead to changes in water uptake in the same way.

The temperature dependencies of the conductivity values for the compositions $SrLa_2ScInO_7$ and $SrLa_2Sc_2O_7$ under dry (filled symbols) and wet (open symbols) air are presented in Figure 5.

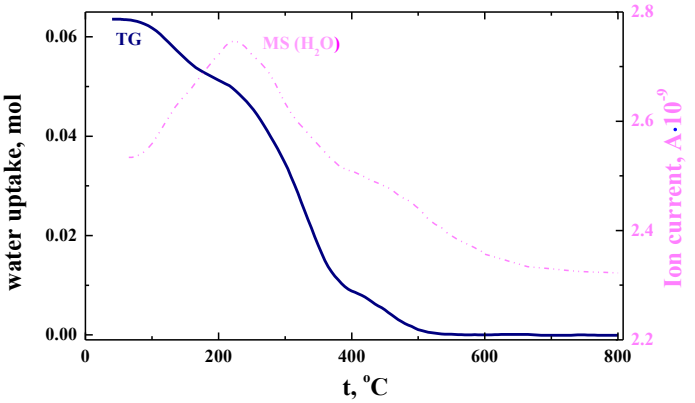

Figure 4 TG- and MS (H_2O)-curves for the hydrated composition $SrLa_2ScInO_7$.

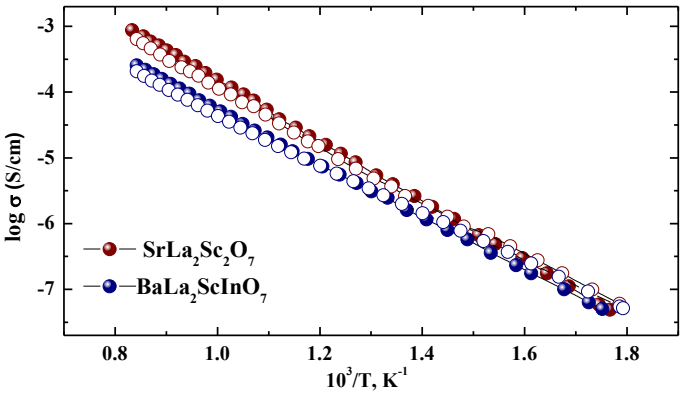

Figure 5 Temperature dependencies of conductivity for the compositions $SrLa_2ScInO_7$ (blue symbols) and $SrLa_2Sc_2O_7$ (red symbols) under dry (filled symbols) and wet (open symbols) air.

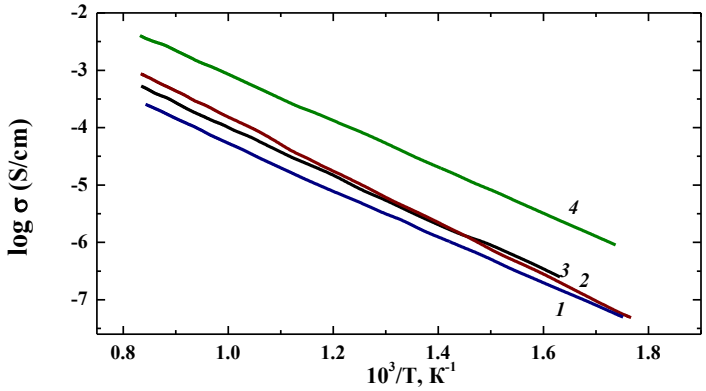

Figure 6 Temperature dependencies of conductivity under dry air for the compositions $SrLa_2ScInO_7$ (1), $SrLa_2Sc_2O_7$ (2), $BaLa_2In_2O_7$ [41] (3), $BaNd_2In_2O_7$ [43] (4).

As can be seen, the electrical conductivity for the composition with two different ions in the B-sublattice of the bilayer perovskite $AA'_2B_2O_7$ ($SrLa_2ScInO_7$) is lower than for the compositions with one type of ions ($SrLa_2Sc_2O_7$). We can assume that the presence of ions of different nature in the same sublattice can lead to a local distortion of the crystal lattice, which in turn can prevent the transfer of ions despite an increase in the lattice parameters. It should be noted that difference in electrical conductivity values decreases with decreasing temperature. The values of activation energy (0.9 eV for $SrLa_2Sc_2O_7$ and 0.8 eV for $SrLa_2ScInO_7$) correlate well with this. The effect of the air humidity starts lower 500 °C which agrees well with TG-data. This allows to say that the proton conductivity contribution occurs in a humid atmosphere at low temperatures. However, the conductivity values are not high. Among bilayer perovskites $AA'_2B_2O_7$ electrical conductivity values increase in the row $SrLa_2ScInO_7$ – $SrLa_2Sc_2O_7$ – $BaLa_2In_2O_7$ – $BaNd_2In_2O_7$ (Figure 6).

Thus, it can be said that the bilayer perovskite $SrLa_2Sc_2O_7$ is not a suitable matrix to modify and obtain new promising proton-conducting materials.

4. Conclusions

In this paper, the possibility of heterovalent and isovalent doping of La and Sc sublattices of bilayer perovskite $SrLa_2Sc_2O_7$ was made for the first time. It was shown that both heterovalent (acceptor and donor) and isovalent doping of the indium sublattice is almost non-existent. The compositions $SrLa_{1.9}M_{0.1}Sc_2O_{6.95}$ (M = Ca, Sr, Ba), $SrLa_2Sc_{1.9}M'_{0.1}O_7$ (M' = In, Gd, Y) and $SrLa_2Sc_{1.9}Ti_{0.1}O_{7.05}$ were non-single phase. The possibility of interaction with water vapours and electrical conductivity were investigated for the single phase composition $SrLa_2ScInO_7$. It was shown that composition $SrLa_2ScInO_7$ introduces a small amount of water (0.06 mol H_2O per mol complex oxide). The proton conductivity contribution occurs in a humid atmosphere at low temperatures. The conductivity values for composition $SrLa_2ScInO_7$ are not high. They increase in the row $SrLa_2ScInO_7$ – $SrLa_2Sc_2O_7$ – $BaLa_2In_2O_7$ – $BaNd_2In_2O_7$. The bilayer perovskite $SrLa_2Sc_2O_7$ is not a suitable matrix to modify and obtain new promising proton-conducting materials.

Supplementary materials

No supplementary materials are available.

Funding

This research was performed according to the budgetary plan of the Institute of High Temperature Electrochemistry and funded by the Budget of Russian Federation.

Acknowledgments

None.

Author contributions

Nataliia Tarasova: Conceptualization; Data curation; Writing – original draft; Writing – review & editing.

Conflict of interest

The authors declare no conflict of interest.

Additional information

Natalia Tarasova, Scopus ID 37047923700.

References

1. Zhang F, Zhu K, Additive Engineering for Efficient and Stable Perovskite Solar Cells Advanced Energy, Materials **10 (131)** (2020) 1902579. https://doi.org/10.1002/aenm.201902579

2. Kwon N, Lee J, Ko MJ, Kim YY, Seo J, Recent progress of eco-friendly manufacturing process of efficient perovskite solar cells, Nano Convergence **10 (1)** (2023) 28. https://doi.org/10.1186/s40580-023-00375-5

3. Liu S, Biju VP, Qi Y, Chen W, Liu Z, Recent progress in the development of high-efficiency inverted perovskite solar cells, NPG Asia Materials **15 (1)** (2023) 27. https://doi.org/10.1038/s41427-023-00474-z

4. Wu T, Qin Z, Wang Y et al., The Main Progress of Perovskite Solar Cells in 2020–2021, Nano-Micro Lett. **13** (2021) 152. https://doi.org/10.1007/s40820-021-00672-w

5. Liu XK, Xu W, Bai S et al., Metal halide perovskites for light-emitting diodes, Nat. Mater. **20** (2021) 10–21. https://doi.org/10.1038/s41563-020-0784-7

6. Li X, Gao X, Zhang X et al., Lead-Free Halide Perovskites for Light Emission: Recent Advances and Perspectives, Advanced Science **8 (4)** (2021) 2003334. https://doi.org/10.1002/advs.202003334

7. Zhang Q, Shang Q, Su R, Do TTH, Xiong Q, Halide Perovskite Semiconductor Lasers: Materials, Cavity Design, and Low Threshold, Nano Letters **21 (5)** (2021) 1903–1914. https://doi.org/10.1021/acs.nanolett.0c03593

8. Liu D, Luo D, Iqbal A.N. et al., Strain analysis and engineering in halide perovskite photovoltaics, Nat. Mater. **20** (2021) 1337–1346. https://doi.org/10.1038/s41563-021-01097-x

9. Dey A, Ye J et al., State of the Art and Prospects for Halide Perovskite Nanocrystals, ACS Nano **15 (7)** (2021) 10775–10981. https://doi.org/10.1021/acsnano.0c08903

10. Li J, Duan J, Yang X, Duan Y, Yang P, Tang Q, Review on Recent Progress of Lead-Free Halide Perovskites in Optoelectronic Applications, Nano Energy **80** (2020) 105526. https://doi.org/10.1016/j.nanoen.2020.105526

11. Sun C, Alonso JA, Bian J, Recent Advances in Perovskite-Type Oxides for Energy Conversion and Storage Applications, Advanced Energy Materials **11 (2)** (2021) 2000459. https://doi.org/10.1002/aenm.202000459

12. Kaur P, Singh K, Review of perovskite-structure related cathode materials for solid oxide fuel cells, Ceramics International **46 (5)** (2020) 5521–55351. https://doi.org/10.1016/j.ceramint.2019.11.066

13. Ding P, Li W, Zhao H, Wu C, Zhao Li, Dong B, Wang S, Review on Ruddlesden-Popper perovskites as cathode for solid oxide fuel cells, J. Phys. Mater. **4 (2)** (2021) 022002. https://doi.org/10.1088/2515-7639/abe392

14. Hanif MB, Rauf S, Motola M, Babar ZUD, Li CJ, Li CX, Recent progress of perovskite-based electrolyte materials for solid oxide fuel cells and performance optimizing strategies for energy storage applications, Materials Research Bulletin **146** (2022) 111612, https://doi.org/10.1016/j.materresbull.2021.111612

15. Kasyanova AN, Zvonareva IA, Tarasova NA, Bi L, Medvedev DA, Shao Z, Electrolyte materials for protonic ceramic electrochemical cells: Main limitations and potential solutions, Mater. Rep. Energy **2** (2022) 100158. https://doi.org/10.1016/j.matre.2022.100158

16. Küngas R, Review – Electrochemical CO_2 Reduction for CO Production: Comparison of Low- And High-Temperature Electrolysis Technologies, Journal of the Electrochemical Society **167 (4)** (2020) https://doi.org/10.1149/1945-7111/ab7099

17. Kamkeng AND, Wang M, Hu J, Du W, Qian F, Transformation technologies for CO2 utilisation: Current status, challenges and future prospects, Chemical Engineering Journal **4091** (2021) 128138. https://doi.org/10.1016/j.cej.2020.128138

18. Younas M, Shafique S, Hafeez A, Javed F, Rehman F, An Overview of Hydrogen Production: Current Status, Potential, and Challenges, Fuel **31615** (2022) 123317. https://doi.org/10.1016/j.fuel.2022.123317

19. Hossain MK, Chanda R, El-Denglawey A., Emrose T, Rahman MT, Biswas MC, Hashizume K, Recent progress in barium zirconate proton conductors for electrochemical hydrogen device applications: A review, Ceramics International **47 (17)** (2021) 23725–237481. https://doi.org/10.1016/j.ceramint.2021.05.167

20. Hanif MB, Rauf S, Abadeen Z et al., Proton-conducting solid oxide electrolysis cells: Relationship of composition-structure-property, their challenges, and prospects, Matter **6 (6)** (2023) 1782–1830. https://doi.org/10.1016/j.matt.2023.04.013

21. Nayak AK, Sasmal A, Recent advance on fundamental properties and synthesis of barium zirconate for proton conducting ceramic fuel cell, Journal of Cleaner Production **386** (2023) 135827. https://doi.org/10.1016/j.jclepro.2022.135827

22. Rasaki SA, Liu C, Lao C, Chen Z, A review of current performance of rare earth metal-doped barium zirconate perovskite: The promising electrode and electrolyte material for the protonic ceramic fuel cells, Progress in Solid State Chemistry **63** (2021) 100325. https://doi.org/10.1016/j.progsolidstchem.2021.100325

23. Hossain MK, Biswas MC, Chanda RK et al. A review on experimental and theoretical studies of perovskite barium zirconate proton conductors, Emergent Mater. **4** (2021) 999–1027, https://doi.org/10.1007/s42247-021-00230-5

24. Vera CYR, Ding H, Peterson D et al., A mini-review on proton conduction of BaZrO3-based perovskite electrolytes, J. Phys. Energy **3** (2021) 032019, https://doi.org/10.1088/2515-7655/acl2ab

25. Fujii K, Esaki Y, Omoto K, Yashima M, Hoshikawa A, Ishigaki T, Hester JR, New Perovskite-Related Structure Family of Oxide-Ion Conducting Materials $NdBaInO_4$, Chem. Mater. **26 (2014)** 2488−2491. https://doi.org/10.1021/cm500776x.

26. Fujii K, Shiraiwa M, Esaki Y, Yashima M, Kim SJ, Lee S, Improved oxide-ion conductivity of $NdBaInO_4$ by Sr doping, J. Mater. Chem. A **3** (2015) 11985. https://doi.org/10.1039/c5ta01336d

27. Troncoso L, Alonso JA, Aguadero A, Low activation energies for interstitial oxygen conduction in the layered perovskites $La_{1+x}Sr_{1-x}InO_{4+d}$, J. Mater. Chem. A **3** (2015) 7797–17803. https://doi.org/10.1039/c5ta03185k

28. Troncoso L, Alonso JA, Fernández-Díaz MT, Aguadero A, Introduction of interstitial oxygen atoms in the layered perovskite $LaSrIn_{1-x}B_xO_{4+\delta}$ system (B=Zr, Ti), Solid State Ion. **282** (2015) 82–87. https://doi.org/10.1016/j.ssi.2015.09.014

29. Ishihara T, Yan Y, Sakai T, Ida S, Oxide ion conductivity in doped $NdBaInO_4$, Solid State Ion. **288** (2016) 262–265. https://doi.org/10.1016/j.ssi.2016.01.011

30. Yang X, Liu S, Lu F, Xu J, Kuang X, Acceptor Doping and Oxygen Vacancy Migration in Layered Perovskite $NdBaInO_4$-Based Mixed Conductors, J. Phys. Chem. C **120** (2016) 6416–6426. https://doi.org/10.1021/acs.jpcc.6b00700

31. Fijii K, Yashima M, Discovery and development of $BaNdInO_4$—A brief review, J. Ceram. Soc. Jpn. **126** (2018) 852–859. https://doi.org/10.2109/jcersj2.18110

32. Troncoso L, Mariño C, Arce MD, Alonso JA, Dual Oxygen Defects in Layered $La_{1.2}Sr_{0.8-x}Ba_xInO_{4+d}$ (x = 0.2, 0.3) Oxide-Ion Conductors: A Neutron Diffraction Study, Materials **12** (2019) 1624. https://doi.org/10.3390/ma12101624

33. Tarasova N, Animitsa I, Galisheva A, Korona D, Incorporation and Conduction of Protons in Ca, Sr, Ba-Doped $BaLaInO_4$ with Ruddlesden-Popper Structure, Materials **12** (2019) 1668. https://doi.org/10.3390/ma12101668

34. Troncoso L, Arce MD, Fernández-Díaz MT, Mogni LV, Alonso JA, Water insertion and combined interstitial-vacancy oxygen conduction in the layered perovskites $La_{1.2}Sr_{0.8-x}Ba_xInO_{4+\delta}$, New J. Chem. **43** (2019) 6087–6094. https://doi.org/10.1039/C8NJ05320K

35. Zhou Y, Shiraiwa M, Nagao M, Fujii K, Tanaka I, Yashima M, Baque L, Basbus JF, Mogni LV, Skinner SJ, Protonic Conduction in the $BaNdInO_4$ Structure Achieved by Acceptor Doping, Chem. Mater. **33** (2021) 2139–2146. https://doi.org/10.1021/acs.chemmater.0c04828

36. Shiraiwa M, Kido T, Fujii K, Yashima M, High-temperature proton conductors based on the (110) layered perovskite BaNdScO4, J. Mat. Chem. A **9** (2021) 8607. https://doi.org/10.1039/D0TA11573H

37. Tarasova NA, Animitsa IE, Galisheva AO, Medvedev DA, Layered and hexagonal perovskites as novel classes of proton-conducting solid electrolytes. A focus review, Electrochem. Mater. Technol. **1** (2022) 20221004. https://doi.org/10.15826/elmattech.2022.1.004

38. Tarasova N, Galisheva A, Animitsa I, Korona D, Davletbaev K, Novel proton-conducting layered perovskite based on $BaLaInO_4$ with two different cations in B-sublattice: Synthesis, hydration, ionic (O^{2+}, H^-) conductivity, International journal of hydrogen energy **47 (44)** (2022) 1897–18982. https://doi.org/10.1016/j.ijhydene.2022.04.112

39. Tarasova N, Galisheva A, Animitsa I, Ba^{2+}/Ti^{4+}-co-doped layered perovskite BaLaInO4: The structure and ionic (O^{2-}, H^+) conductivity. Int. J. Hydrog. Energy **46** (2021) 16868–16877. https://doi.org/10.1016/j.ijhydene.2021.02.044

40. Tarasova N, Animitsa I, Materials $A^{II}LnInO_4$ with Ruddlesden-Popper Structure for Electrochemical Applications: Relationship between Ion (Oxygen-Ion, Proton) Conductivity, Water Uptake, and Structural Changes, Materials **15 (1)** (2022) 114. https://doi.org/10.3390/ma15010114

41. Tarasova N, Galisheva A, Animitsa I, Belova K, Egorova A, Abakumova E, Medvedev D, Layered Perovskites $BaM_2In_2O_7$ (M = La, Nd): From the Structure to the Ionic (O^{2-}, H^+) Conductivity, Materials **15** (2022) 3488. https://doi.org/10.3390/ma15103488

42. Tarasova N, Layered Perovskites $BaLn_nIn_nO_{3n+1}$ (n = 1, 2) for Electrochemical Applications: A Mini Review, Membranes **13** (2023) 34. https://doi.org/10.3390/membranes13010034

43. Tarasova N, Bedarkova A, Animitsa I, Abakumova E, Cation and oxyanion doping of layered perovskite $BaNd_2In_2O_7$: oxygen-ion and proton transport, International journal of hydrogen energy **48 (59)** (2023) 22522–22530. https://doi.org/10.1016/j.ijhydene.2022.11.172

44. Tarasova N, Bedarkova A, Animitsa I, Abakumova E, Gnatyuk V, Zvonareva I, Novel Protonic Conductor $SrLa_2Sc_2O_7$ with Layered Structure for Electrochemical Devices, Materials **15** (2022) 8867. https://doi.org/10.3390/ma15248867

45. Shannon RD, Revised effective ionic radii and systematic studies of interatomic distances in halides and chalcogenides, Acta Cryst. **A32** (1976) 751–767. https://doi.org/10.1107/S0567739476001551